

HETEROCYCLES, Vol. 83, No. 10, 2011, pp. 2329 - 2336. © 2011 The Japan Institute of Heterocyclic Chemistry
Received, 14th June, 2011, Accepted, 5th August, 2011, Published online, 8th August, 2011
DOI: 10.3987/COM-11-12281

THE GLASSY MESOMORPHISM OF UNSYMMETRICAL BIPEDAL LIQUID CRYSTALS DERIVED FROM TETRATHIAFULVALENE AND CHOLESTEROL

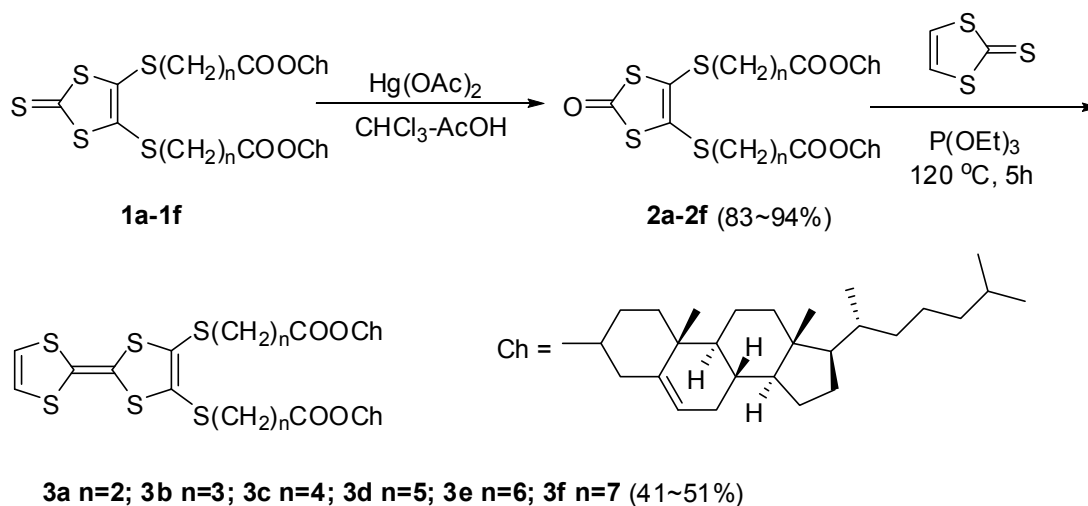
Ningjuan Zheng, Han Wang, Ruibin Hou, and Bingzhu Yin*

Key Laboratory of Natural Resources of Changbai Mountain & Functional Molecules (Yanbian University), Ministry of Education, Yanji 133002, China
e-mail: zqcong@ybu.edu.cn

Abstract – 1,3-dithiole-2-ones attached two cholesteryl through two ω -thio-alkanoyloxy spacer of varying length were easily transformed to the appropriate TTF-based unsymmetrical bipedal by cross-coupling reaction in net triethyl phosphite. All of tetrathiafulvalene-based bipedals exhibit mesogenic phases in a wide temperature region, no crystallization but vitrifying to form glassy mesogens during cooling from the isotropic melt.

Tetrathiafulvalene (TTF) derivatives have played a pivotal role in the development of organic materials for optoelectronic application due to their excellent electron-donating properties.¹ The transport properties of these materials are clearly dependent on the molecular architecture in the solid state and so a wide variety of substituents have been introduced at the periphery of the TTF core in order to achieve a suitable solid-state organization.² In this respect, a possible approach is based on the preparation of mesogenic compounds. In particular, glassy liquid crystals (GLCs) hold a fast and good orientation, which can be readily processed into macroscopically ordered solid films.³ Although a considerable number of TTF derivatives have so far been synthesized, there are only a few reports describing TTF derivatives with mesomorphic properties⁴ and consequently, it is not yet possible to establish structure-property relationships for this family of compounds. Very recently, we reported that the symmetrical tetrapedals derived from TTF and cholesterol exhibited smectic and/or hexagonal columnar phases, which depended on the length of spacers.⁵ In order to create new TTF-based mesomorphic states, a series of cholesteryl with various alkyl chain lengths was introduced onto one side of the TTF core. Here, we report the synthesis and mesomorphic properties of TTF-based unsymmetrical bipedals **3a-3f** containing two cholesteryls, together with the electron donating property of TTF central core.

The structures and synthetic route of TTF-based bipedals were shown in **Scheme 1**. The starting 3-dithiole-2-thiones (**1a-1f**) attached two cholesteryl through two ω -thioalkanoyloxy spacer of varying length were easily transformed to the appropriate ketones (**2a-2f**) using conventional methods in high yields. The cross-coupling reaction of **2a-2f** with 3-dithiole-2-thione yielded the TTF-based unsymmetric bipedals (**3a-3f**) in net triethyl phosphate at 120 °C.



Scheme 1. Synthesis route of bipedal liquid crystals

The phase sequences and phase structures of **3a-3f** were investigated by polarized-light optical microscopy (POM), differential scanning calorimetry (DSC), and small-angle X-ray scatterings (SAXS). All the synthesized bipedals exhibit mesophases in a wide temperature range including room temperature and no crystallization but vitrifying to form glassy mesogen during cooling from the isotropic melt. The **3a-3e** exhibited only one mesophase in a wide temperature region. Only **3f** with the longest spacer showed two phase transitions in heating as well as in cooling cycle (Table 1). For example, **3c** ($n=4$) exhibited a liquid crystalline phase at a melting state (34.1 °C), which was transformed to an isotropic phase at 80.5 °C (Figure 1a). On slow cooling of **3c** from the isotropic liquid to liquid crystalline phase at 77.7 °C, a sanded texture was observed by POM experiment, which was transformed to glassy state at ca. 27.5 °C during cooling (Figure 2a). The SAXS of **3c** measured at cooling to 40 °C displayed three sharp reflections with d spacings of 519, 260, and 170 nm, which were in the ratio of 3:2:1 and agreed well with (100), (200), and (300) reflections of a lamellar packing structure (Figure 1b). Considering the layer thickness (5.19 nm) obtained from the X-ray diffraction pattern is much larger than the estimated molecular length (2.94 nm by CPK model) and the S \cdots S interaction between TTF segments, bimolecule arrangement in lamellar structure is expected, in which TTF segments interdigitated to fill the space. The small-angle X-ray diffraction patterns of **3a**, **3b** and **3d** also displayed similar Bragg diffraction peaks

corresponding to the long spacing or layer reflections in the small-angle region and thus also index to a lamellar structure. Considering the similarity of the optical textures with those of **3a-3b** and **3d-3e**

Table 1. Phase transition temperature and enthalpy changes of **3a-3f** determined by DSC in the second cooling scan^a and their cyclic voltammetry vs SCE in CH₂Cl₂ (10⁻³ M).

Compound	Transition temperature (°C) and enthalpy changes (J·g ⁻¹), Heating cycle/Cooling cycle	E ¹ _{1/2} /V	E ² _{1/2} /V
TTF ^b		0.340	0.710
3a	g 50.1 (1.1) S _A 96.9 (3.7) I / I 97.2 (4.0) S _A -- g	0.487	0.947
3b	g 33.4 (0.5) S _A 73.6 (2.6) I / I 76.1 (3.2) S _A -- g	0.467	0.924
3c	g 34.1 (0.8) S _A 80.5 (5.0) I / I 77.7 (5.3) S _A -- g	0.448	0.904
3d	g 31.0 (0.8) S _A 77.7 (4.4) I / I 75.5 (4.7) S _A -- g	0.438	0.896
3e	g 23.9 (0.9) S _A 69.6 (2.5) I / I 71.9 (2.9) S _A -- g	0.439	0.895
3f	g 22.3 (2.04) S _A 57.1 (0.8) Col 74.7 (0.7) I / I 74.9 (0.8) Col 62.1 (1.3) S _A -- g	0.437	0.895

^ag = glass state, S_A = smectic A, Col = columnar, I = isotropic. ^bref 6

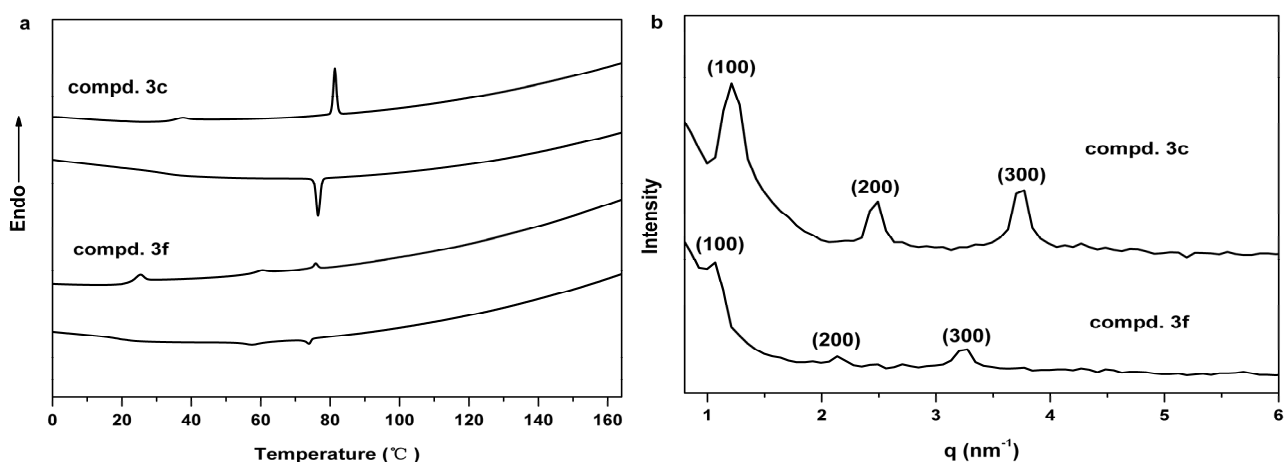


Figure 1. (a) DSC traces (10 °C/min) recorded during the second heating and the second cooling scan of **3c** and **3f**; (b) X-ray diffraction patterns of **3c** and **3f** plotted against $q = 4\pi \sin\theta/\lambda$ measured at 40 °C.

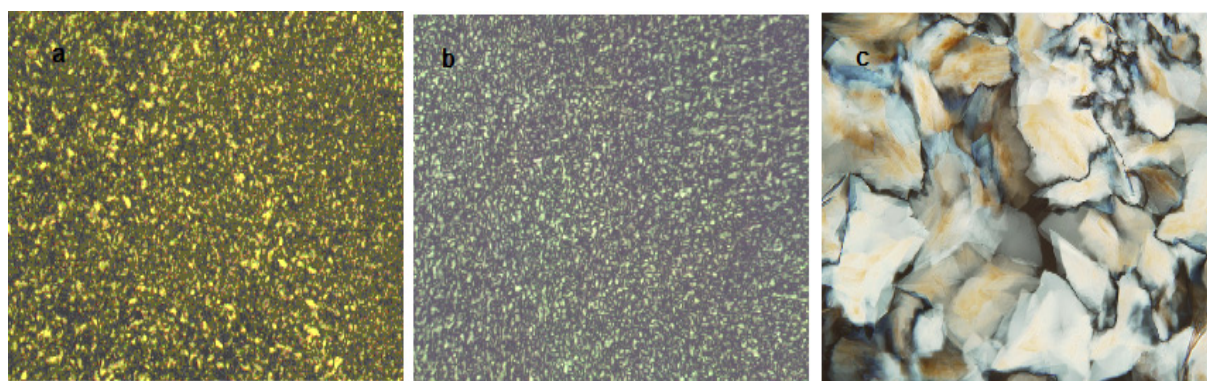


Figure 2. Optical polarized micrographs (40×) of the texture exhibited by (a) the S_A phase of **3c** at 60 °C; (b) The S_A phase of **3f** at 50 °C; (c) The Col phase of **3f** at 60 °C.

could also be indexed to lamellar arrangement. The compound **3f** ($n=7$) with the longest spacer is unique in that it displays two mesophases at 22.3 °C and 57.1 °C, followed by transformation to an isotropic phase at 74.7 °C (Figure 1a). Upon cooling from the isotropic liquid, a mosaic texture was observed by POM experiment (Figure 2c). To identify the detailed phase structure, SAXS studies were performed but no useful peak in the lower Bragg angle region was observed at high temperature region (60-70 °C). Considering the phase sequences and optical texture, it probably is a columnar phase. The longer spacer is favorable to a columnar structure packing because it probably provide a bigger disk to avoid the crowding between cholesteryl groups.⁵ On further cooling to 62.1 °C, the columnar phase gradually transformed to another mesophase, the typical sanded texture appeared and its disordered systems induce vitrification rather than crystallization during cooling (Figure 2b). The X-ray diffraction pattern of **3f** measured at cooling to 40 °C displays three sharp reflections corresponding to spacing of 5.88, 2.94, and 1.96 nm in the small-angle region (Figure 1b). They are in the ratio of 3:2:1 and could be indexed as (100), (200), and (300) reflections of a lamellar packing structure. Considering the layer thickness (5.88 nm) obtained from the X-ray diffraction pattern, bimolecule arrangement in lamellar structure is also expected.

To evaluate electron donating property of TTF-based bipedal **3a-3f**, the cyclic voltammetry (CV) measurements were performed in a dry CH_2Cl_2 solution of Bu_4NBF_4 (0.1 M) with a scan rate of 100 mV s^{-1} at room temperature (Table 1 and Figure 3a). The bipedal **3a-3f** showed two reversible single-electron oxidation peaks at ~ 0.49 and ~ 0.95 V, corresponding to the formation of radical cations and dication of TTF, respectively, indicating two sequential reversible one-electron transfer steps. The oxidation potentials of **3a-3f** were higher than those of TTF probably due to the existence of electron-withdrawing

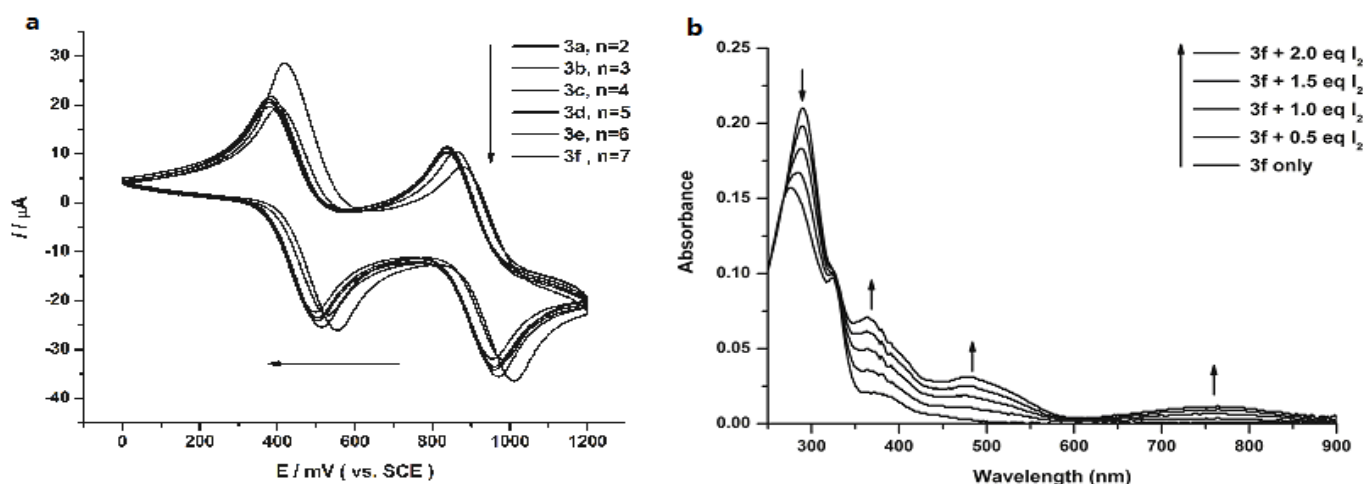


Figure 3. (a) CVs of **3a-3f** (5×10^{-4} M) in 0.1 M Bu_4NPF_6 in CH_2Cl_2 (9:1, v/v) at 0.1 V s^{-1} ; (b) UV-vis absorption spectral change of **3f** (10^{-5} M) in CH_2Cl_2 upon stepwise addition of I_2 .

ester linkages in the distance. Therefore, as the methylene spacer lengthened (from $n = 2$ to $n = 5$), the halfwave potential was anodic shifted in a regular manner.

To investigate the potential of these structures to act as a conducting architecture, chemical oxidation of **3f** in a CH_2Cl_2 solution (10^{-5} M) was conducted with stepwise addition of I_2 . Upon stepwise addition of I_2 (0.5→2.0 equiv) to a CH_2Cl_2 solutions of **3f**, three new CT absorption bands appeared at 364, 482 and 734 nm (Figure 3b). The absorptions at 364 and 482 nm was assigned to an intramolecular electron transfer of radical cation, $3f^{+\bullet}$, while the absorption band at 734 nm was due to an intermolecular electron transfer of the π -dimer of **3f** dications.⁷

In summary, a series of bipedal liquid crystals based on TTF and cholesterol was synthesized by cross-coupling reaction of 1,2-dithiol-2-ones bearing two cholesteryl side chains with 1,2-dithiol-2-thione. All of the TTF-based bipedals exhibit mesophases in a wide temperature range including room temperature and no crystallization but vitrifying to form glassy mesogen during cooling from the isotropic melt. These liquid crystals, in combination with the glassy mesogen and excellent electron-donating properties of TTF, may provide new opportunities in the development of soft materials.

EXPERIMENTAL

NMR spectra were recorded in CDCl_3 with a Bruker AV-300 Spectrometer (300 MHz for ^1H and 75 MHz for ^{13}C) and chemical shifts were referenced relative to tetramethylsilane ($\delta_{\text{H}}/\delta_{\text{C}} = 0$). MALDI-TOF-MS was performed on a Shimadzu Axima CFRTM Plus using a 1,8,9-anthracenetriol (DITH) matrix. IR spectra were recorded on a Shimadzu FT-IR Prestige-21 instrument (KBr pressed disc method). UV-vis spectra were recorded on a Hitachi U-3010 spectrophotometer in CH_2Cl_2 (10^{-5} M). Cyclic voltammetric studies were carried out on a Potentiostat/Galvanostat 273A instrument in CH_2Cl_2 (10^{-3} M) and 0.1 M Bu_4PF_6 as the supporting electrolyte. Counter and Working electrodes were made of Pt and Glass-Carbon, respectively, and the reference electrode was calomel electrode (SCE). A Perkin-Elmer Pyris Diamond differential scanning calorimeter was used to determine the thermal transitions, the heating and cooling rates were controlled to 10 °C/min. An Olympus BX51-P optical polarized microscope (40×) was used to observe the thermal transitions and to analyze the anisotropic texture. X-ray scattering measurements were performed in transmission mode with Philips PW 1700 X-ray diffractometer. Compounds **1a-1f** were synthesized according to our literature method.⁵

Typical synthetic procedure for **2**

Mercuric acetate (9.81 mmol) was added in one portion to suspension of **1** (3.27 mmol) in a mixture of CHCl_3 (60 mL) and glacial acetic acid (20 mL), causing the initially yellow solution to change to white within 2 min. The resulting white suspension was stirred at room temperature for 5 h, whereupon the

white precipitate was filtered and washed thoroughly with CH_2Cl_2 . The combined organic phase was washed with saturated aqueous NaHCO_3 solution, H_2O and dried over MgSO_4 . Evaporation of the solvent in vacuum and the residue was purified by column chromatography (silica gel, CH_3Cl) to give **2**.

2a. White slimy solid, Yield: 90%, mp 26.99 °C (by DSC). ^1H - NMR (CDCl_3): δ 0.68-2.33 (m, 86H, aliphatic and cholesteric protons are overlapped), 2.66 (t, $J = 7.4$ Hz, 4H), 3.01 (t, $J = 7.4$ Hz, 4H), 4.56-4.73 (m, 2H), 5.39 (brs, 2H); FT-IR (KBr, cm^{-1}): 2947 (C-H), 1734 (C=O, ester), 1672 (C=O), 1190 (C-O). Anal. Calcd for $\text{C}_{63}\text{H}_{98}\text{O}_5\text{S}_4$: C, 71.14; H, 9.29. Found: C, 70.80; H, 9.57.

2b. White slimy solid, Yield: 94%, mp 19.53 °C (by DSC). ^1H - NMR (CDCl_3): δ 0.68-2.31 (m, 90H, aliphatic and cholesteric protons are overlapped), 2.46 (t, $J = 7.4$ Hz, 4H), 2.91 (t, $J = 7.4$ Hz, 4H), 4.56-4.73 (m, 2H), 5.38-5.40 (m, 2H); FT-IR (KBr, cm^{-1}): 2949 (C-H), 1732 (C=O, ester), 1678 (C=O), 1171 (C-O). Anal. Calcd for $\text{C}_{65}\text{H}_{102}\text{O}_5\text{S}_4$: C, 71.51; H, 9.42. Found: C, 71.42; H, 9.75.

2c. White slimy solid, Yield: 92%, mp 10.89 °C (by DSC). ^1H NMR (300 MHz, CDCl_3): δ 0.67-2.34 (m, 98H, aliphatic and cholesteric protons are overlapped), 0.86 (s, 6H), 2.89 (t, $J = 7.0$ Hz, 4H), 4.58-4.76 (m, 2H), 5.38-5.46 (m, 2H); FT-IR (KBr, cm^{-1}): 2947 (C-H), 1730 (C=O, ester), 1668(C=O), 1171 (C-O). Anal. Calcd for $\text{C}_{67}\text{H}_{106}\text{O}_5\text{S}_4$: C, 71.86; H, 9.54. Found: C, 71.60; H, 9.55.

2d. White slimy solid, Yield: 87%, mp 8.03 °C (by DSC). ^1H NMR (300 MHz, CDCl_3): δ 0.68-2.38 (m, 102H, aliphatic and cholesteric protons are overlapped), 2.89 (t, $J = 7.2$ Hz, 4H), 4.55-4.75 (m, 2H), 5.38-5.42 (brs, 2H); FT-IR (KBr, cm^{-1}): 2947 (C-H), 1732 (C=O, ester), 1668(C=O), 1171 (C-O). Anal. Calcd for $\text{C}_{69}\text{H}_{110}\text{O}_5\text{S}_4$: C, 72.20; H, 9.66. Found: C, 71.91; H, 9.35.

2e. White slimy solid, Yield: 90%, mp 6.03 °C (by DSC). ^1H NMR (300 MHz, CDCl_3): δ 0.67-2.32 (m, 106H, aliphatic and cholesteric protons are overlapped), 2.83 (t, $J = 7.2$ Hz, 4H), 4.59-4.62 (m, 2H), 5.36-5.37 (m, 2H); FT-IR (KBr, cm^{-1}): 2936 (C-H), 1732 (C=O, ester), 1670 (C=O), 1171 (C-O). Anal. Calcd for $\text{C}_{71}\text{H}_{114}\text{O}_5\text{S}_4$: C, 72.52; H, 9.77. Found: C, 72.41; H, 10.02.

2f. White slimy solid (Yield: 95%), mp 4.10 °C (by DSC). ^1H - NMR (CDCl_3): δ 0.68-2.40 (m, 110H, aliphatic and cholesteric protons are overlapped), 2.84 (t, $J = 7.2$ Hz, 4H), 4.52-4.64 (m, 2H), 5.36-5.40 (m, 2H); FT-IR (KBr, cm^{-1}): 2949 (C-H), 1732 (C=O, ester), 1668 (C=O), 1172 (C-O); Anal. Calcd for $\text{C}_{73}\text{H}_{118}\text{O}_5\text{S}_4$: C, 72.82; H, 9.88. Found: C, 73.00; H, 9.56.

Typical synthetic procedure for **3**

2 (0.5 mmol) and 1,3-dithiol-2-thione (0.5 mmol) was added to $\text{P}(\text{OEt})_3$ (5 mL) and the suspension was heated to 120 °C, causing dissolution within 1 min, leaving a yellow reaction mixture. The mixture was stirred for 5 h at 120 °C, cooled to room temperature. Addition of MeOH gave a yellow solid, which was filtered, washed with MeOH, and dried in vacuo. The products were purified by column chromatography (silica gel, CH_2Cl_2 :PE = 3:1; v/v) to give a yellow solid. The solid was recrystallized from CH_2Cl_2 /

n-Hexane gave **3**.

3a. Yellow solid (Yield: 43%). ^1H NMR (300 MHz, CDCl_3): δ 0.68-2.11 (m, 82H, aliphatic and cholesteric protons are overlapped), 2.33 (d, $J = 7.4$ Hz, 4H), 2.66 (t, $J = 7.1$ Hz, 4H), 3.06 (t, $J = 7.4$ Hz, 4H), 4.64 (m, 2H), 5.38 (brs, 2H), 6.33 (s, 2H); MS (EI): m/z (%) 1149 (M^+ , 100); FT-IR (KBr, cm^{-1}): 2943 (C-H), 1730 (C=O), 1179 (C-O); Anal. Calcd for $\text{C}_{66}\text{H}_{100}\text{O}_4\text{S}_6$: C, 68.94; H, 8.77. Found: C, 68.71; H, 9.06.

3b. Yellow solid (Yield: 44%). ^1H NMR (300 MHz, CDCl_3): δ 0.68-2.08 (m, 86H, aliphatic and cholesteric protons are overlapped), 2.32 (d, $J = 7.45$ Hz, 4H), 2.45 (t, $J = 7.2$ Hz, 4H), 2.87 (t, $J = 7.4$ Hz, 4H), 4.62 (m, 2H), 5.38 (brs, 2H), 6.31 (s, 2H); MS (EI): m/z (%) = 1177 (M^+ , 100); FT-IR (KBr, cm^{-1}): 2936 (C-H), 1732 (C=O), 1172 (C-O). Anal. Calcd for $\text{C}_{68}\text{H}_{104}\text{O}_4\text{S}_6$: C, 69.34; H, 8.90. Found: C, 69.50; H, 8.66.

3c. Yellow solid (Yield: 43%). ^1H NMR (300 MHz, CDCl_3): δ 0.69-2.31 (m, 100H, aliphatic and cholesteric protons are overlapped), 2.83 (t, $J = 7.0$ Hz, 4H), 4.62 (m, 2H), 5.39 (brs, 2H), 6.31 (s, 2H); MS (EI): m/z (%) = 1205 (M^+ , 100); FT-IR (KBr, cm^{-1}): 2947 (C-H), 1730 (C=O), 1169 (C-O). Anal. Calcd for $\text{C}_{70}\text{H}_{108}\text{O}_4\text{S}_6$: C, 69.71; H, 9.03. Found: C, 69.90; H, 9.01.

3d. Yellow solid (Yield: 42%). ^1H NMR (300 MHz, CDCl_3): δ 0.68-2.32 (m, 102H, aliphatic and cholesteric protons are overlapped), 2.81 (t, $J = 7.2$ Hz, 4H), 4.62 (m, 2H), 5.38 (brs, 2H), 6.32 (s, 2H); MS (EI): m/z (%) = 1233 (M^+ , 100). FT-IR (KBr, cm^{-1}): 2945 (C-H), 1734 (C=O), 1170 (C-O). Anal. Calcd for $\text{C}_{72}\text{H}_{112}\text{O}_4\text{S}_6$: C, 70.08; H, 9.15. Found: C, 69.89; H, 9.34.

3e. Yellow solid (Yield: 51%). ^1H NMR (300 MHz, CDCl_3): δ 0.67-2.32 (m, 106H, aliphatic and cholesteric protons are overlapped), 2.81 (t, $J = 7.2$ Hz, 4H), 4.59-4.62 (m, 2H), 5.36-5.38 (m, 2H), 6.32 (s, 2H); MS (EI): m/z (%) = 1260 (M^+ , 100). FT-IR (KBr, cm^{-1}): 2936 (C-H), 1732 (C=O), 1171 (C-O). Anal. Calcd for $\text{C}_{74}\text{H}_{116}\text{O}_4\text{S}_6$: C, 70.42; H, 9.26. Found: C, 70.30; H, 9.36.

3f. Yellow solid (Yield: 46%). ^1H NMR (300 MHz, CDCl_3): δ 0.68-2.32 (m, 110H, aliphatic and cholesteric protons are overlapped), 2.84 (t, $J = 7.2$ Hz, 4H), 4.62 (m, 2H), 5.37 (brs, 2H), 6.32 (s, 2H); MS (EI): m/z (%) = 1289 (M^+ , 100). FT-IR (KBr, cm^{-1}): 2930 (C-H), 1736 (C=O), 1175 (C-O). Anal. Calcd for $\text{C}_{76}\text{H}_{120}\text{O}_4\text{S}_6$: C, 70.75; H, 9.38. Found: C, 70.50; H, 9.54.

ACKNOWLEDGEMENTS

This work was supported by the National Science Foundation of China (No. 21062022) and the Specialized Research Fund for the Doctoral Program of Higher Education (Grant No. 20102201110001).

REFERENCES

1. (a) M. R. Bryce, *Chem. Soc. Rev.*, 1991, **20**, 355; (b) M. R. Bryce, *J. Mater. Chem.*, 1995, **5**, 1481; (c)

- J. W. Goodby, I. M. Saez, S. J. Cowling, V. Gortz, M. Draper, A. W. Hall, S. Sia, G. Cosquer, S.-E. Lee, and E. P. Raynes, *Angew. Chem. Int. Ed.*, 2008, **47**, 2754.
2. R. Andreu, J. Barberá, J. Garín, J. Orduna, J. L. Serrano, T. Sierra, P. Leriche, M. Sallé, A. Riou, M. Jubault, and A. J. Gorgues, *Mater. Chem.*, 1998, **8**, 881.
 3. H. P. Chen, D. Katsis, J. C. Mastrangelo, S. H. Chen, and S. D. Jacobs, *Adv. Mater.*, 2000, **12**, 1283.
 4. (a) M. Katsuhara, I. Aoyagi, H. Nakajima, T. Mori, T. Kambayashi, M. Ofuji, Y. Takanishi, K. Ishikawa, H. Takezoe, and H. Hosono, *Synth. Met.*, 2005, **149**, 219; (b) X. Gao, W. Wu, Y. Liu, S. Jiao, W. Qiu, G. Yu, L. Wang, and D. Zhu, *J. Mater. Chem.*, 2007, **17**, 736; (c) R. A. Bissell, N. Boden, R. J. Bushby, C. W. G. Fishwick, E. Holland, B. Movaghar, R. J. Bushby, and G. Ungar, *Chem. Commun.*, 1998, 113; (d) A. González, J. I. Segura, and N. Martín, *Tetrahedron Lett.*, 2000, **41**, 3083; (e) R. Andreu, J. Garín, J. Orduna, J. Barberá, J. L. Serrano, T. Sierra, M. Sallé, and A. Gorgues, *Tetrahedron*, 1998, **54**, 3895; (f) L. Wang, K.-U. Jeong, and M.-H. Lee, *J. Mater. Chem.*, 2008, **18**, 2657; (g) I. C. Pintre, J. L. Serrano, M. Blanca, C. L. Folcia, J. Etxebarria, F. Goc, D. B. Amabilino, J. Puigmartí-Luis, and E. Gomar-Nadald, *Chem. Commun.*, 2008, 2523; (h) J. Martínez-Perdiguero, I. Alonso, J. Ortega, C. L. Folcia, J. Etxebarria, I. Pintre, M. B. Ros, and D. B. Amabilino, *Phys. Rev. E*, 2008, **77**, 020701; (i) I. Alonso, J. Martínez-Perdiguero, C. L. Folcia, J. Etxebarria, J. Ortega, I. C. Pintre, and M. B. Ros, *Phys. Rev. E*, 2008, **78**, 041701.
 5. R. B. Hou, Z. G. Huang, K. L. Zhong, L.-Y. Jin, and B. Z. Yin, *Tetrahedron*, 2011, **67**, 1238.
 6. D. J. Green, *J. Chem. Soc., Chem. Commun.*, 1977, **6**, 161.
 7. (a) L. Huchet, S. Akoudad, E. Levillain, and J. Roncali, *J. Phys. Chem., B*, 1998, **102**, 7776; (b) H. Spanggaard, J. Prehn, M. B. Nielsen, E. Levillain, M. Allain, and J. Becher, *J. Am. Chem. Soc.*, 2000, **122**, 9486.